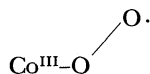


Physical and Chemical Properties of Mononuclear Cobalt Dioxygen Complexes with Tetraimidazolyl-Substituted Pyridine Chelates

Seizo TAMAGAKI, Yutaka KANAMARU, Masanori UENO, and Waichiro TAGAKI*
Department of Bioapplied Chemistry, Faculty of Engineering, Osaka City University,
Sugimoto 3, Sumiyoshi-ku, Osaka 558
(Received May 7, 1990)

A new class of mononuclear superoxocobalt complexes containing four equal imidazolyl-donors and one pyridyl-donor per cobalt(II) ion was prepared and their chemical and physical properties were compared with those of cobalt(II) Schiff-base type dioxygen complexes.

Since the first recognition of oxygen fixation by the Co^{II} complex of a synthetic chelate, *N,N'*-disalicylideneethylenediamine (salen),¹⁾ reversible oxygenations with mononuclear peroxo complexes of low valent transition metals such as Ir^{I} , Rh^{I} , Co^{I} , and Ni^0 have been reported, in which the two oxygen atoms are equidistant from the metal.^{2,3)} Meanwhile, a wide variety of binuclear μ -peroxo complexes have been synthesized^{2,4)} and it has been found that in the presence of pyridine and imidazole reversible dioxygenation is possible with analogs of Co^{II} (salen) complexes such as Co^{II} (3-methoxysalen)^{5,6)} and Co^{II} (acacen), [*N,N'*-ethylenebis(4-imino-2-pentanonato)]-cobalt(II),⁷⁾ forming the corresponding dioxygen complexes, whose structures were characterized as paramagnetic mononuclear superoxocobalt(III) complexes being in equilibrium with the corresponding μ -peroxo complexes;



Metal dioxygen complexes are important for (1) a better understanding of the role of hemoglobin and myoglobin in biological systems;⁸⁾ (2) development of efficient catalysts for oxygenation of organic substrates;⁹⁾ (3) use in separating dioxygen from air or removing traces of dioxygen from inert gases.¹⁰⁾ In this work we have synthesized a new class of imidazolyl-methyl-substituted pyridine chelates (hereinafter this

will be referred to as tip) and have studied the physical and chemical properties of their cobalt dioxygen complexes as well as their utility for oxygenations of phenols to fully characterize them.

Experimental

Materials. Solvents used in this study were purified via standard procedures by distillation, and only the central fraction was used. Special grade cobalt nitrate and perchlorate as the hydrates were purchased from Kishida Chemical Co. and used without further purification. Tetraimidazolylmethyl-substituted pyridine ligands, tip (tip(a)—tip(d)), were prepared by the procedure previously described with minor modifications.¹¹⁾ A 500 mL flask was flame-dried. After cooling it with a stream of nitrogen, 200 mL of freshly distilled, dry THF containing 0.1 mol of *N*-alkylimidazole was added with cooling to Dry Ice/acetone temperature (-78°C) under nitrogen. Sixty-three mL of a 1.6 M solution of butyllithium in hexane ($M=\text{mol dm}^{-3}$) was injected dropwise to that solution using a glass syringe. To assure the completion of the reaction, the reaction temperature was maintained at the same temperature for additional one hour. To the solution diethyl 2,6-pyridinedicarboxylate (5.6 g, 0.024 mol) in 50 mL of THF was added dropwise. The reaction temperature was then allowed to rise to room temperature. After the mixture was stirred for 4 h, water was added and the organic solvent was stripped off. Continuous extraction of the water layer with ethyl acetate gave a white crystalline solid, tip(a), which was recrystallized from CHCl_3 -hexane.

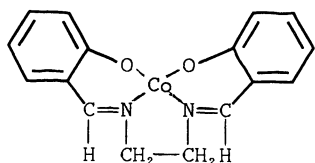
Tip(a): Yield 54.3%; mp $181\text{--}184^\circ\text{C}$; NMR (CDCl_3) $\delta=3.09$ (16H, s, CH_3), 6.10 (2H, s, OH), 6.68 (4H, s, Im-2H), 6.89 (4H, s, Im-3H), 7.13 (1H, m, py-4H), 7.52 (2H, m, py-3,5H).

Tip(b) was purified by recrystallization from benzene-hexane after evaporation of the THF, extraction with CHCl_3 and evaporation of the CHCl_3 .

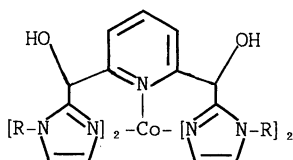
Tip(b): Yield 48.7%; mp $164\text{--}166^\circ\text{C}$; NMR (CDCl_3) $\delta=0.7\text{--}1.6$ (28H, m, $(\text{CH}_2)_2\text{CH}_3$), 3.58 (8H, t, N-CH₂), 6.04 (2H, s, OH), 6.79 (8H, s, Im-CH=CH), 7.23—7.70 (3H, m, py-3,4,5H).

With tip(c) and tip(d), the CHCl_3 extracts were subjected to preparative TLC and the solids obtained were recrystallized from hexane (yield 34.7% mp $107\text{--}108^\circ\text{C}$) and from benzene-hexane (yield 45.1%; mp $178\text{--}179^\circ\text{C}$), respectively.

Tip(d): 2.92 (12H, s, OCH_3), 6.60 (2H, s, OH), 6.78, 6.91 (8H, d, CH=CH), 7.1—7.8 (3H, m, py-3,4,5H).



Co(salen)



[Co(tip(a—e))] ²⁺;

R: CH_3 (tip(a))

$n\text{-C}_4\text{H}_9$ (tip(b))

$n\text{-C}_8\text{H}_{17}$ (tip(c))

CH_3OCH_2 (tip(d))

CH_3CH_2 (tip(e))

Isolation of [Co(tip)(O₂)]²⁺ and Its Reaction Product.

Tip(a) (0.1 mmol) was mixed at -30°C with an equimolar amount of $\text{Co}(\text{NO}_3)_2 \cdot 6\text{H}_2\text{O}$ in 25 mL of nitromethane, and tip(b) or tip(c) in 25 mL of CH_2Cl_2 , and bubbling of oxygen gave immediately dark-red solutions of $[\text{Co}(\text{tip})(\text{O}_2)]^{2+}$ complexes, which were entirely stable to a further reaction at such a low temperature in solution. Evaporation of the solvent below -30°C under a reduced pressure of 1 mmHg (1 mmHg=133.322 Pa) afforded dark-red colored solids. $[\text{Co}(\text{tip(a)})(\text{O}_2)]^{2+}$ salt: yield 98%. Meanwhile, when tip(a) (0.1 mmol) was added with stirring to $\text{Co}(\text{NO}_3)_2 \cdot 6\text{H}_2\text{O}$ (0.1 mmol) in 10 mL of acetone at room temperature under oxygen, dark-red solids began to precipitate. (The $[\text{Co}(\text{tip})]^{2+}$ complex itself did not precipitate out under nitrogen.) After 1 h, the precipitates were filtered, washed with acetone, and dried under vacuum, affording an analytical sample.

$[\text{Co}(\text{tip(a)})(\text{O}_2)](\text{NO}_3)_2(\text{H}_2\text{O})_2$: Yield 91%; decomp $140-143^{\circ}\text{C}$.

Anal. Calcd for $\text{C}_{23}\text{H}_{29}\text{N}_{11}\text{O}_{12}\text{Co}$: C, 38.88; H, 4.11; N, 21.69%. Found: C, 39.11; H, 4.43; N, 21.27%.

When tip(a) (0.2 mmol) was mixed with $\text{Co}(\text{NO}_3)_2 \cdot 6\text{H}_2\text{O}$ (0.2 mmol) in 25 mL of acetonitrile under oxygen at room temperature, complete bleaching of the solution was effected in 2 days. The solution was then evaporated to dryness and the residue was washed thoroughly with acetonitrile. Yield 90% in weight; decomp. $187-190^{\circ}\text{C}$. Because of its tendency to decompose when subjected to recrystallization or precipitation, it is not possible to obtain the product in the pure form. The elemental analysis of this product gave no constant value within analytical accuracy with samples taken from different runs, but most likely agrees with a dimeric complex $[\text{Co}_2(\text{tip(a)})_2(\text{O}_2)](\text{NO}_3)_4$.

Isolation of $[\text{Co}(\text{tip(a)})(\text{base})]^{2+}$ Complexes. To stoichiometric amounts of tip(a) and $\text{Co}(\text{NO}_3)_2 \cdot 6\text{H}_2\text{O}$ (0.3 mmol each) was added a large excess of a desired base, for example, *N*-methylimidazole (Meim) under nitrogen in 25 mL of nitromethane. Rotary evaporation of the solvent provided slightly pink powders in 96% yield, which were precipitated from nitromethane/ CH_2Cl_2 /benzene in the presence of excess 1-methylimidazole.

$[\text{Co}(\text{tip(a)})(\text{Meim})](\text{NO}_3)_2(\text{H}_2\text{O})_2$: decomp. $245-250^{\circ}\text{C}$. Anal. Calcd for $\text{C}_{27}\text{H}_{35}\text{N}_{13}\text{O}_{10}\text{Co}$: C, 42.65; H, 4.61; N, 23.95%. Found: C, 42.33; H, 4.8; N, 24.45%.

Oxygen Uptake Experiment. The amount of oxygen absorbed by $[\text{Co}(\text{tip(a)})]^{2+}$ was determined at 20°C according to the Warburg's manometry.¹²⁾ K_{O_2} is the equilibrium constant defined according to the equation below:

$$\text{LCo}^{2+} + \text{O}_2 \rightleftharpoons \text{LCoO}_2^{2+} \quad K_{\text{O}_2} = \frac{[\text{LCoO}_2^{2+}]}{[\text{LCo}^{2+}] \times P_{\text{O}_2}}$$

where P_{O_2} is the oxygen pressure in mmHg. The full equilibration was presumed to be quickly attained.

Kinetic Procedure for Disappearance of the Superoxocobalt Complexes. All experiments have been done at 25°C under 1 atm oxygen pressure. The progress of disappearance of a cobalt oxygen complex was followed by monitoring the disappearance of absorption at 505 nm. As the superoxo complex is formed in relatively fast equilibrium, its disappearance reaction was monitored soon after injecting a needed volume of acetonitrile solution of $\text{Co}(\text{NO}_3)_2$ into 3 mL of a tip acetonitrile (0.5 mM each) in a 1 cm UV-cell

capped with a rubber septum.

Electrochemistry. Cyclic voltammetric measurements were performed under nitrogen using a NP-IR 1000 potentiostat/galvanostat. Special grade acetonitrile was distilled from P_4O_{10} . Tetrabutylammonium perchlorate was used as the supporting electrolyte. To 20 mL of an acetonitrile solution containing 3 mM tip(b) and 0.1M Bu_4NClO_4 was added 100 μL of 0.6 M $\text{Co}(\text{ClO}_4)_2$ under nitrogen. The measurements utilized a platina wire working electrode, a platina wire auxiliary electrode, and an Ag/AgCl reference electrode in a one-compartment cell. The cyclic voltammogram of $[\text{Co}(\text{tip(b)})]^{2+}$ thus obtained is given in Fig. 1a. Figure 1b shows a cyclic voltammogram in the presence of 5-fold excess of pyridine. The $E_{1/2}$ values were estimated from cyclic voltammograms using the expression $E_{1/2} = (E_p + E_{p/2})/2$ where E_p is the peak potential and $E_{p/2}$ is the half peak potential.

ESR Spectrum. The solid cobalt-oxygen complex was placed in an ESR tube, after which the tube was degassed. The ESR signals were recorded at -196°C on a JES-ME-3X spectrometer with an X-band microwave unit and 100 KHz field modulation.

Oxygenation of 2,4-Di-*t*-butylphenol. To a red solution of an equimolar mixture of $\text{Co}(\text{ClO}_4)_2 \cdot 6\text{H}_2\text{O}$ (9.15 mg, 0.025 mmol, 0.5 M) and tip(b) (15.68 mg) in 50 mL of various solvents was added 1.0 mmol (206 mg) of 2,4-di-*t*-butylphenol. The reaction was allowed to proceed under oxygen at room temperature for 44 h. For determination of product yields, the solvent was rotary evaporated at room temperature, and then the residue was subjected to thin-layer chromatography with Kiesel gel G/ CHCl_3 , affording 3,5-di-*t*-butyl-*o*-benzoquinone and 3,3',5,5'-tetra-*t*-butyl-1,1'-biphenyl-2,2'-diol (hereafter designated as biphenyl-2,2'-diol): Mp $193-195^{\circ}\text{C}$; NMR (CDCl_3) $\delta=1.3$ (36H, d, *t*-butyl), 5.08 (2H, s, Ar-OH), 6.94-7.21 (4H, m, Ar-H); MS (70 eV) m/z (rel intensity) 410 (M^+ ; 100), 395(52), 339(20), 283(15), and 190(48). Determination of the quinone yield was made spectrophotometrically at 400 nm ($\epsilon=1704$) in MeCN within experimental error of $\pm 3\%$.¹³⁾ The yields in various solvents are collected in Table 2.

Oxygenation of 2,6-Di-*t*-butylphenol. To a solution of 0.05 mmol each of tip(b) and $\text{Co}(\text{NO}_3)_2 \cdot 6\text{H}_2\text{O}$ in 25 mL solvents was added 2,6-*t*-butylphenol (103 mg, 0.5 mmol). The reaction was continued with gentle stirring at room temperature under oxygen. After 24 h, the solvent was stripped off under reduced pressure at room temperature and the residue was subjected to preparative thin-layer chromatography using benzene-hexane (1:1) as eluant giving two products. The yields were determined spectrophotometrically. 2,6-Di-*t*-butyl-*p*-benzoquinone (*p*-BQ): 450 nm ($\epsilon=39$)¹⁴⁾ and a diphenoquinone (DPQ): 260 nm ($\epsilon=4056$).¹⁵⁾

Kinetic Method for Oxygenation. Reactions were performed under the conditions specified in Fig. 8. Unless otherwise noted, the concentration of 3,5-di-*t*-butylphenol was in 10-fold excess over the catalyst. In a typical experiment, a septum-capped flask containing pure O_2 -saturated acetone solution of $\text{Co}(\text{NO}_3)_2$ and tip(b) was maintained at 25°C . Reactions were initiated by injecting the phenol dissolved in acetone. A 75 μL aliquot of the reaction mixture was then transferred by a microsyringe into a UV cell containing 3 mL of acetonitrile. The increasing absorbance at 400 nm characteristic of the product quinone

was monitored every 30 minutes.

Instrumentals. NMR, IR, and UV spectra were obtained on a Hitachi R-24B, a Nihon Bunko A-202 infrared spectrometer, and a Hitachi 220 spectrophotometer, respectively.

Results and Discussion

Physical Properties of $[\text{Co}(\text{tip}(\text{b}))]^{2+}$ and Their Oxygen Complexes. In cyclic voltammograms of oxygen-free $[\text{Co}(\text{tip}(\text{b}))]^{2+}$ and $[\text{Co}(\text{tip}(\text{b}))(\text{base})]^{2+}$ complexes a single quasi-reversible redox wave associated with cobalt(II/III) couples appears at negative potentials. (Fig. 1a and 1b). The redox-potentials are summarized in Table 1. There is no distinct correlation between

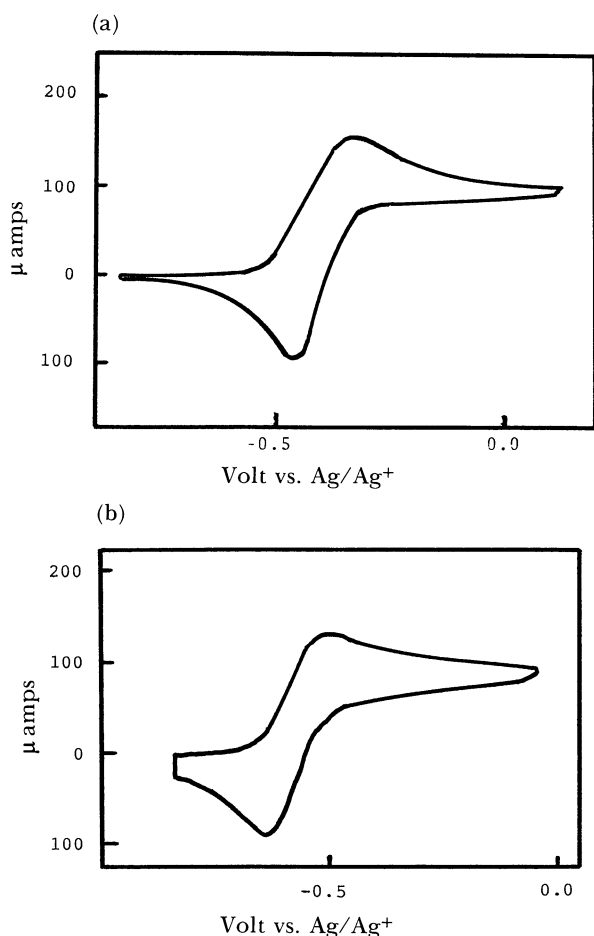


Fig. 1. Cyclic voltammograph of a) $[\text{Co}(\text{tip}(\text{b}))]^{2+}$ and b) $[\text{Co}(\text{tip}(\text{b})(\text{py}))]^{2+}$. Scan rate 50 mV^{-1} . E versus Ag/Ag^+ . Counter anion: ClO_4^- in MeCN .

Table 1. Redox Potentials of $[\text{Co}(\text{tip}(\text{b}))(\text{base})]^{2+}$ Complexes^{a)}

Base	$\text{p}K_a$	$E_{1/2}/\text{V}$ vs. Ag/AgCl
Pyridine	5.27	-0.51
Piperidine	11.3	-0.54
1-Methylimidazole	7.25	-0.65
Butylamine	10.61	-0.66

a) Conditions: $[\text{tip}(\text{b})]=[\text{Co}(\text{ClO}_4)_2]=3 \text{ mM}$; $[\text{Base}]=15 \text{ mM}$; $[\text{Bu}_4\text{NClO}_4]=0.1 \text{ M}$ in MeCN at 27°C .

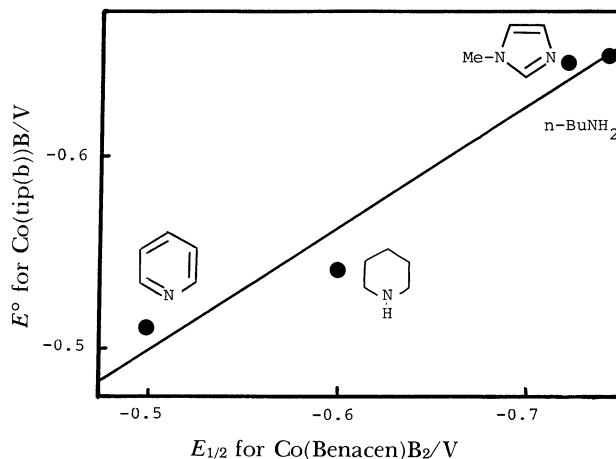
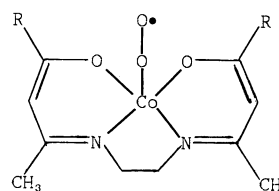


Fig. 2. Correlation of $E_{1/2}$ for $[\text{Co}(\text{tip}(\text{b}))(\text{B})]^{2+}$ with that for $\text{Co}(\text{benacen})\text{B}_2$. $[\text{Co}(\text{tip}(\text{b}))^{2+}]=3 \text{ mM}$; $[\text{B}]=15 \text{ mM}$; $[\text{Bu}_4\text{NClO}_4]=0.1 \text{ M}$ in MeCN at 27°C .

$E_{1/2}$ values and $\text{p}K_a$ values of bases, probably because piperidine, a secondary cyclic amine, is sterically hindered and *N*-methylimidazole is a good π -electron donating base. In Fig. 2 is shown a plot of the redox potentials of $[\text{Co}(\text{tip}(\text{b}))]^{2+}$ vs. those of $\text{Co}(\text{benacen})$ complex, $[\text{N},\text{N}'\text{-ethylenebis(3-imino-1-phenyl-1-butanonato)}]\text{cobalt(II)}$, in the presence of various bases.¹⁶⁾ The $E_{1/2}$ values of $[\text{Co}(\text{tip}(\text{b}))(\text{B})]^{2+}$ ($\text{B}=\text{base}$) are linearly related to those of $\text{Co}(\text{benacen})(\text{B})_2$ with a



$R = \text{Ph}$: $\text{Co}(\text{benacen})(\text{O}_2)$

$R = \text{Me}$: $\text{Co}(\text{acacen})(\text{O}_2)$

slope of 0.66. The slope close to 0.5 is simply interpreted by considering that the latter has one more additional base than the former. Figure 3 shows a plot of the absorbance against cobalt nitrate concentrations under an atmosphere of dioxygen gas in acetonitrile, keeping the concentration of $\text{tip}(\text{b})$ fixed. A nearly linear correlation up to a 1:1 molar ratio of cobalt nitrate to the chelate demonstrates that the chelate and cobalt ion form a 1:1 complex.

In our preliminary report, it was established that addition of dioxygen to $[\text{Co}(\text{tip}(\text{a}))]^{2+}$ in acetonitrile is apparently reversible since a stream of nitrogen bubbling into the solution at ambient temperature resulted in the disappearance of its original red color characteristic of the $[\text{Co}(\text{tip}(\text{O}_2))]^{2+}$ complex.¹¹⁾ Subsequent bubbling of oxygen through the solution restored the red color and, hence, the complex was formulated as a mononuclear superoxocobalt(III) complex. The elemental analysis for $[\text{Co}(\text{tip}(\text{a})(\text{O}_2)]^{2+} \cdot 2\text{NO}_3^-$ supports the validity of the proposed

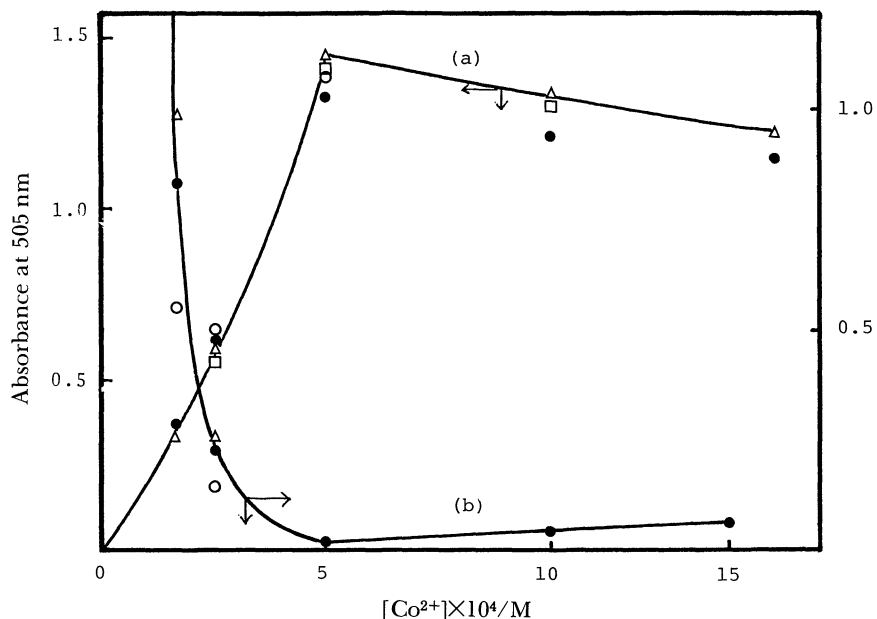
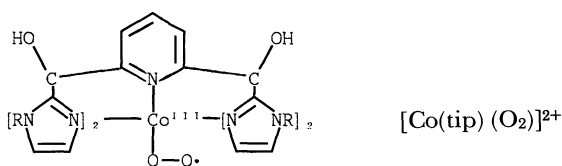


Fig. 3. Effects of altering concentrations of $\text{Co}(\text{NO}_3)_2$ on the formation (a) and disappearance (b) of $[\text{Co}(\text{tip})(\text{O}_2)]^{2+}$ complexes under oxygen in MeNO_2 at 25°C , the tip concentration being fixed constant at 0.5 mM. \circ : tip(a); Δ : tip(b); \square : tip(c); \bullet : tip(e).



structure.

The apparent extinction coefficient at 505 nm of the superoxocobalt complex thus formed is $\epsilon = 1.4 \times 10^3$ and $1.9 \times 10^3 \text{ M}^{-1} \text{ cm}^{-1}$ in acetonitrile and water, respectively, but the observed small reversible oxygen binding constant ($\log K_{\text{O}_2} \text{ mm}^{-1} = -4.1, -4.0, \text{ and } -3.9$ in water, acetonitrile, and nitromethane, respectively, at 20°C) indicates that only a portion of $[\text{Co}(\text{tip}(\text{b}))]^{2+}$ is oxygenated in solution; hence, the real extinction coefficient is $\epsilon = 2.5 \times 10^4$ in water. The K_{O_2} value is roughly the same in magnitude as that of $\text{Co}(\text{benacen})(\text{py})$ in toluene ($\log K_{\text{O}_2} = -1.36 \text{ mm}^{-1}$ at -31°C ; -4.4 at 20°C (extrapolated))¹⁶ and nearly 3-order of magnitude smaller than that of $\text{Co}(\text{salen})(\text{py})$ ($\log K_{\text{O}_2} = -1.05, 20^\circ\text{C}$).¹⁷ The comparable oxygen-binding stabilities for $[\text{Co}(\text{tip})]^{2+}$ and $\text{Co}(\text{benacen})(\text{py})$ reflect a similarity in their reducing ability; $E_{1/2} = -0.51 \text{ V}$ for $[\text{Co}(\text{tip})(\text{py})]^{2+}$ and -0.50 V (vs. SCE) for $\text{Co}(\text{benacen})(\text{py})$.¹⁸

The immediate formation of the superoxocobalt complex was observed as soon as $\text{Co}(\text{NO}_3)_2$ was added to an oxygen-saturated solution of a tip ligand, then followed by its slow disappearance. In Fig. 3 a plot of rate constants for the disappearance of absorbance at 505 nm in nitromethane is also displayed, showing that the rate is significantly dependent on changing

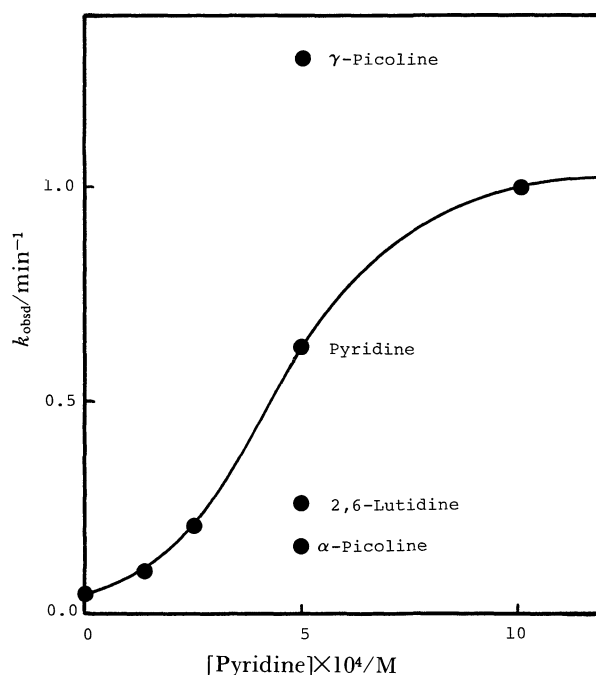
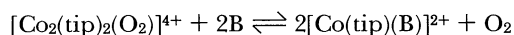


Fig. 4. Effect of changing concentrations of pyridine bases on the rate of disappearance of $[\text{Co}(\text{tip}(\text{c}))(\text{O}_2)]^{2+}$ under oxygen in MeNO_2 at 25°C . $[\text{tip}(\text{c})] = [\text{Co}(\text{NO}_3)_2] = 0.5 \text{ mM}$.

concentrations of the metal ion. In particular, the use of a large excess of the chelate vs. metal ion causes rapid loss of the superoxocobalt complex. This is interpreted as due to interception of $[\text{Co}(\text{tip}(\text{b}))]^{2+}$ by free imidazolyl chelate (tip(b)) to make a new stable

$[\text{Co}(\text{tip}(\text{b}))]^{2+}$ -tip(b) adduct. In fact, as one can see in Fig. 4, a simple base, pyridine or *N*-methylimidazole (Meim), was also found to bring about facile disappearance of the superoxo complex to form the $[\text{Co}(\text{tip})]^{2+}$ -base complex. In order to confirm this interpretation, we performed product analysis using tip(a) as the ligand under two extreme conditions; without added pyridine (or 1-methylimidazole) the reaction produced a slightly pink-colored solid, which evolved gas when heated to $>150^\circ\text{C}$ (140°C) in a capillary tube, while, addition of a large excess of pyridine (Meim) afforded a white solid which melted out at $258\text{--}265^\circ\text{C}$ ($235\text{--}240^\circ\text{C}$) without gas evolution and, when dissolved in solvents, exhibited at 505 nm an absorption band characteristic of the superoxo complex. These observations strongly support that the former is the dimer $[\text{Co}_2(\text{tip}(\text{a}))_2(\text{O}_2)]^{4+}$ and the latter is the adduct $[\text{Co}(\text{tip}(\text{a}))(\text{B})]^{2+}$. When the former was reacted with excess pyridine or when the latter was dissolved in nitromethane under oxygen, the $[\text{Co}(\text{tip})]^{2+}$ was present as a mixture of $[\text{Co}_2(\text{tip})_2(\text{O}_2)]^{4+}$ and $[\text{Co}(\text{tip})(\text{B})]^{2+}$ in either case. Thus, they are interconvertible with each other. However, the equilibrium below lies so far to the left.



The rate of disappearance of the superoxocobalt complex itself is strongly solvent-dependent, and the kinetic orders with regard to the complex concentrations are changing from zero-order in THF to first-order in acetone, dichloromethane, nitromethane, and *t*-butyl alcohol (the rate increases along this solvent series), and to second-order in ethyl acetate, chlorobenzene, benzene, *o*-tolunitrile, nitrobenzene, benzonitrile, acetonitrile, and 1,2-dimethoxyethane (the rate increases in this order) (Fig. 5). As can be seen in, for example, Fig. 6, we could find no simple relationship between initial rates and any solvent properties like dielectric constant, steric bulkiness, polarity, donor number, and degree of oxygen saturation etc., which we could not determine. The irregularity might be due to involvement of several comparable equilibria, which contribute to the overall rate in a complicated way. However, in contrast to the suggestion by Martell and co-workers that $\text{Co}(\text{benacen})$ and $\text{Co}(\text{porphyrin})$ superoxo complexes are more favored in nonpolar solvents such as toluene, the $[\text{Co}(\text{tip})]^{2+}$ and O_2 1:1 complex is destabilized either in low or highly polar solvents. Furthermore, this $[\text{Co}(\text{tip})]^{2+}$ - O_2 system is very interesting, since it can exist even in an aqueous solvent; to date, no superoxocobalt(III) complexes in aqueous solution at room temperature have been reported in the literature.^{2,19)}

In the meantime, the superoxo complex $[(\text{Co}(\text{tip}(\text{a}))(\text{O}_2)]^{2+}$ in the solid state was dark-red and so stable toward deoxygenation at room temperature even

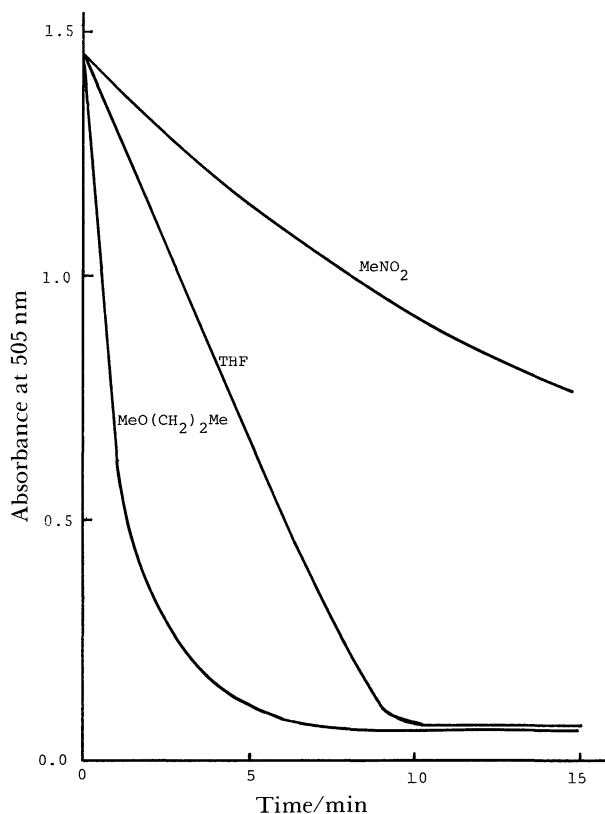


Fig. 5. Time courses of disappearance of absorption due to $[\text{Co}(\text{tip}(\text{c}))(\text{O}_2)]^{2+}$ in various solvents. $[\text{tip}(\text{c})] = [\text{Co}(\text{NO}_3)_2] = 0.5 \text{ mM}$.

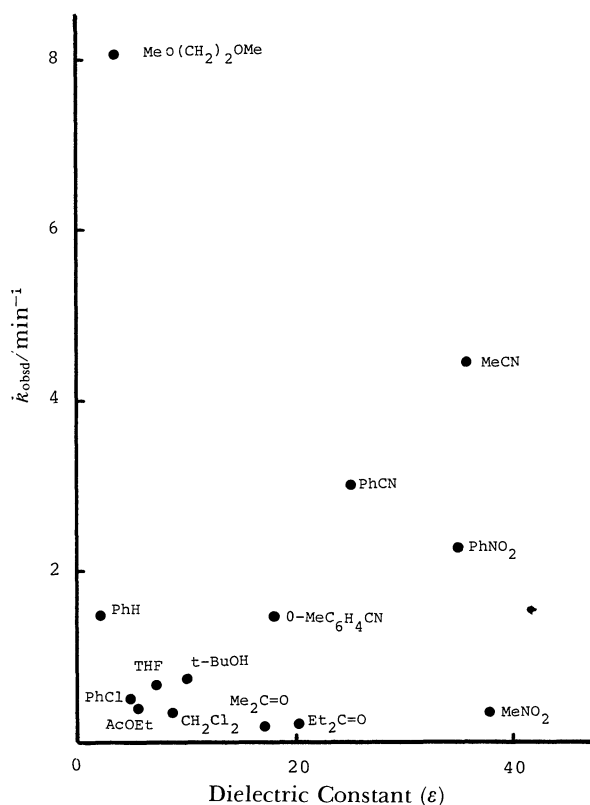


Fig. 6. Influence of solvent change on rate of disappearance of $[\text{Co}(\text{tip}(\text{c}))(\text{O}_2)]^{2+}$. Counter anion: NO_3^- .

under a reduced pressure (1 mmHg). However, heating it for one hour at 140 °C in vacuo results in loss of the color. Upon its exposure to air at room temperature for one day the decolorized complex takes up dioxygen and the original red color is restored. Thus, addition of oxygen to the cobalt–tip(a) complex is apparently reversible. In the reported case of brown-colored oxygenated Co(salen),²⁰ heating it at 100 °C forms red solids. As is revealed by Table 2, the shorter the ligand alkyl-chain length, the higher is the decolorization temperature and the melting point of the superoxo complex. This follows the same order as the melting points of the ligands themselves. The extent of recovery of [Co(tip(a))(O₂)]²⁺ complex was measured at 505 nm to be 54% on each deoxygenation–oxygenation cycle. This recovery extent is almost the same both in the solid and liquid states.

Figure 7 displays the ESR spectrum of [Co(tip(a))(O₂)](NO₃)₂ in the solid state at liquid nitrogen temperature, where eight equivalent hyperfine-splitt-

ing signals with low intensity due to ⁵⁹Co (*I*=7/2) can be observed. Just analogous spectral patterns were reported for Co(acacen)(py)(O₂)²¹ in a toluene matrix at –58 °C and [Co(CN)₅(O₂)]^{3–,22} Co(NO₃)₂ and [Co(tip(a))(py)]NO₃)₂ exhibited no ESR signals owing probably to their electron configurations of high spin states.

Oxygenations of Phenols. There are a number of reports on the oxygenations of sterically hindered

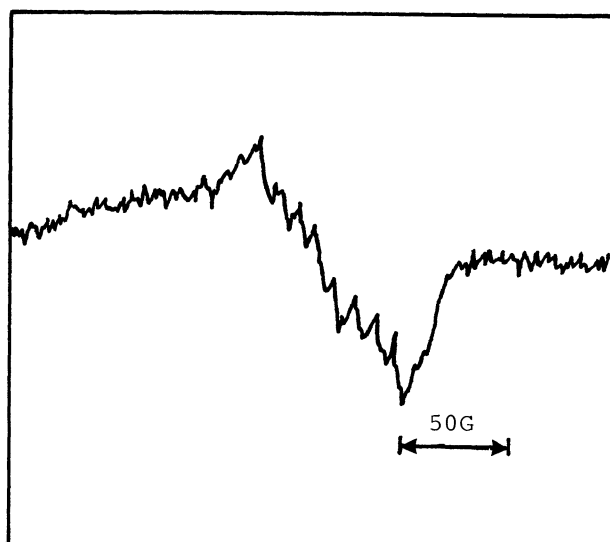


Fig. 7. ESR spectrum of [Co(tip(a))(O₂)]²⁺ in the solid state at –196 °C. Counter anion: NO₃[–].

Table 2. Decolorization Temperatures and Melting Points of [Co(tip)(O₂)]²⁺ Complexes^{a)}

Substituent on imidazolyl group	Decolorization temperature ^{b)} /°C	Melting point
		°C
CH ₃	140	236–254
<i>n</i> -C ₄ H ₉	100	160–165
<i>n</i> -C ₈ H ₁₇	<100	110–125

a) Counter anion: NO₃[–]. b) Under 1 mmHg.

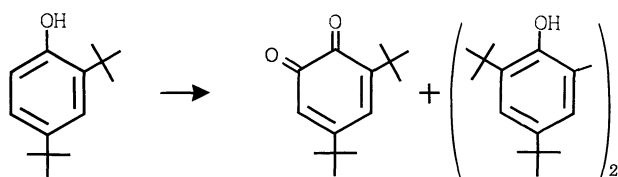
Table 3. Product Yields for Oxygenation of 2,4-Di-*t*-butylphenol with in situ Generated [Co(tip(b))]²⁺ Catalyst

Catalyst	Solvent	Quinone yield/% (±3%)		Biphenyl-2,2'-diol yield/% (±2%) 24 h	Recovered ^{d)} yield/% 24 h
		44 h ^{a)}	24 h ^{b)}		
[Co(tip(b))] ²⁺	MeNO ₂	39	89		
	Me ₂ C=O		85	6	3
			82 ^{c)}	11	Trace
	MeCN	38	63	7	15
			66 ^{c)}	4	15
	CH ₂ Cl ₂	16	23	10	50
	<i>t</i> -BuOH		42		
	DMF	14	6.9		
	MeOH	8.6	6.0	11	77
	CHCl ₃		5.5	10	66
[Co ₂ (tip(b)) ₂ (O ₂) ₂] ⁴⁺	MeO(CH ₂) ₂ OMe		0		
	MeCN		34 ^{c)}	2	58
			3.2 ^{c)}	8.3	72
Co(salen)	MeOH		10.4		
	CH ₂ Cl ₂ ²⁴⁾			100	
	CH ₂ Cl ₂ ²⁴⁾		>85		

Conditions: 2,4-di-*t*-butylphenol 1 mmol; solvent 50mL; under O₂ at room temperature. a) tip(b) 0.025 mmol; Co(ClO₄)₂ 0.025 mmol. b) tip(b) 0.1 mmol; Co(ClO₄)₂ 0.1 mmol. c) Co(NO₃)₂ was used. d) A blank denotes that a yield was not determined. e) tip(b) 0.2 mmol; Co(NO₃)₂ 0.2 mmol; the phenol 1 mmol under N₂.

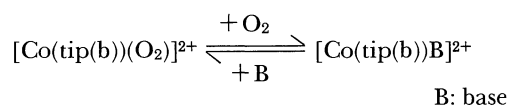
phenols; for instance, 2,4-di-*t*-butylphenol was selectively oxidized with Co(salen) catalyst to the corresponding quinone in DMF and to 3,3',5,5'-tetra-*t*-butyl-1,1'-biphenyl-2,2'-diol (biphenyl-2,2'-diol) in dichloromethane or methanol.^{23,24} In the present study the [Co(tip(b))]²⁺ complex was tested as catalyst for oxygenations of two typical phenols.

The reaction of 2,4-di-*t*-butylphenol catalytically gave rise to 3,5-di-*t*-butyl-*o*-benzoquinone (*o*-BQ) together with biphenyl-2,2'-diol, irrespective of the nature of used solvents (Table 3), without accompanying oxidative cleavage of the aromatic ring as with MnCl₂.²⁵ However, the yield was largely dependent on the solvent employed; generally, nonpolar solvents



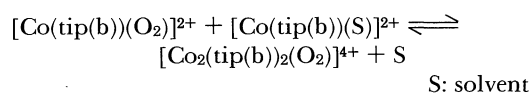
are least effective. Highly polar solvents such as methanol or *N,N*-dimethylformamide led to poorer yields than moderately polar solvents such as nitromethane, acetone, or acetonitrile. This seems to reflect an absolutely low concentration of the reaction-triggering superoxocobalt complexes in those solvents, probably because a [Co(tip(b))]²⁺-solvent adduct rather than the superoxo complex predominantly exists, such

as was observed when basic pyridines were added. As a result, a poorer yield of the *o*-BQ was obtained.



B: base

As is demonstrated in the same table or Fig. 8, the dimeric μ -peroxo complex retains considerable activity under the identical conditions although it is less effective than the in situ generated oxygen complex. This is because, even if the μ -peroxo species itself is inactive, the active superoxo species is produced from it according to the back-reaction of the equilibrium below.



S: solvent

The following tentative mechanism, being consistent with the above observations and reported literature results, completes the sequence of events, where LCo denotes chelated cobalts, H-PH a di-*t*-butylphenol, and PH \cdot and PH⁻ a phenoxyl radical and phenolate ion, respectively.

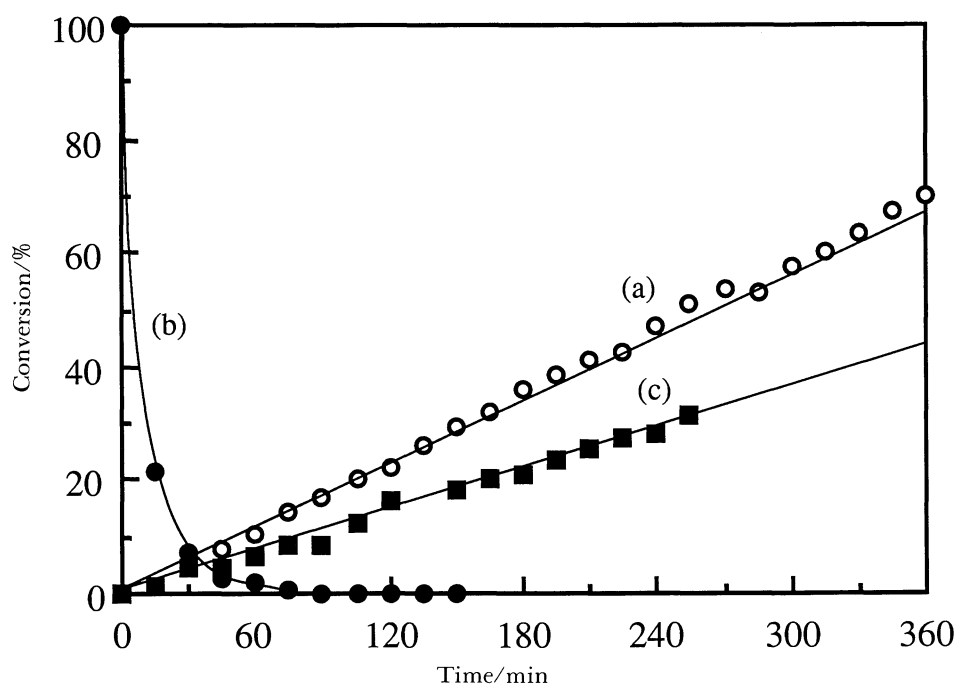
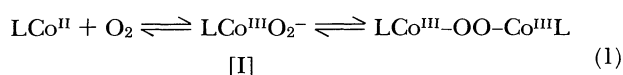
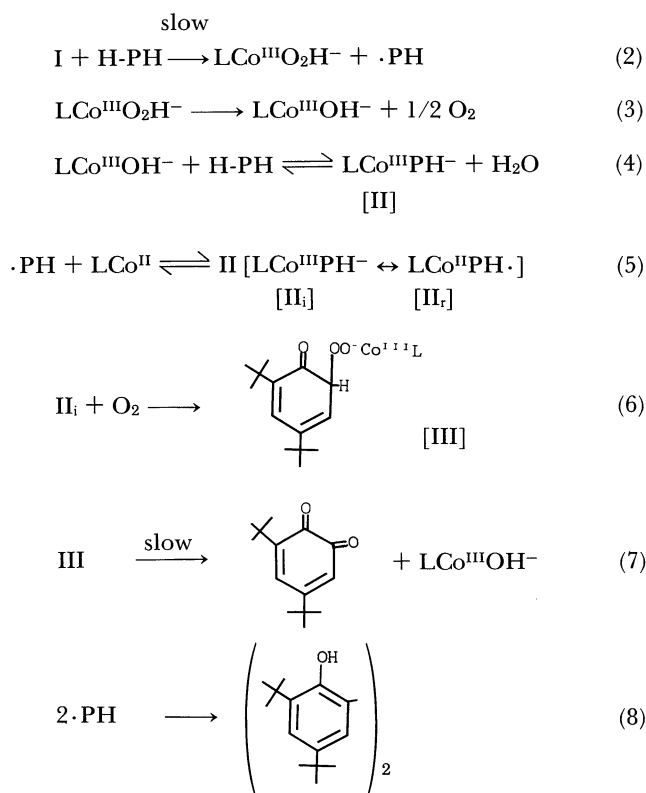


Fig. 8. Time-%conversion profiles for increasing quinone in oxygenation of 2,4-di-*t*-butylphenol using (a) in situ generated [Co(tip(b))(O₂)]²⁺ and (c) [Co₂(tip(b))₂(O₂)]⁴⁺ and for (b) decreasing [Co(tip(b))(O₂)]²⁺ in Me₂CO under oxygen. [Co(NO₃)₂]= [tip(b)]=2.0×10⁻³ M, [phenol]=2.0×10⁻² M.



At first, the reaction sequence appears to be triggered by abstraction of the hydrogen atom of the phenol by the superoxocobalt complex yielding the hydrogen-peroxocobalt complex (Eq. 2), which decomposes to yield a hydroxocobalt complex and oxygen (Eq. 3). Then, the hydroxo complex abstracts the proton from the phenol to form the phenolato LCo^{III} complex (II) with resonance forms II_i and II_r (Eqs. 4 and 5); the ionic form (II_i) would be favored in polar solvents such as acetonitrile and acetone to eventually produce *o*-BQ by reacting with molecular oxygen in its ortho-position (Eq. 6 followed by Eq. 7), while the radicalish form (II_r), which is expected to be favored in nonpolar solvents, is thought to be in equilibrium with the phenoxyl free radical (Eq. 5). The increasing stability of the phenolato complex in a polar solvent, accordingly, resulted in a higher proportion of the quinone vs. the radical coupling product, biphenyl-2,2'-diol, and vice versa in nonpolar solvents, as was observed. A similar metal-phenolate interaction has been proposed by Nishinaga²⁶⁾ and Que²⁷⁾ for an explanation of quinone formations.

Nishinaga et al. have kinetically studied the closely related oxidation in detail using 4-substituted 2,6-di-*t*-butylphenol and Co(salpr) and have proposed a similar mechanism which involves a fast superoxo complex formation followed by the rate-determining phenolic hydrogen atom abstraction (Eqs. 1 and 2).²³⁾ A comparison of kinetic curves (a) and (b) in Fig. 8 shows, however, that the conversion of 2,4-di-*t*-butylphenol to *o*-BQ continued to increase linearly with time up to 80% completion, while the superoxo-

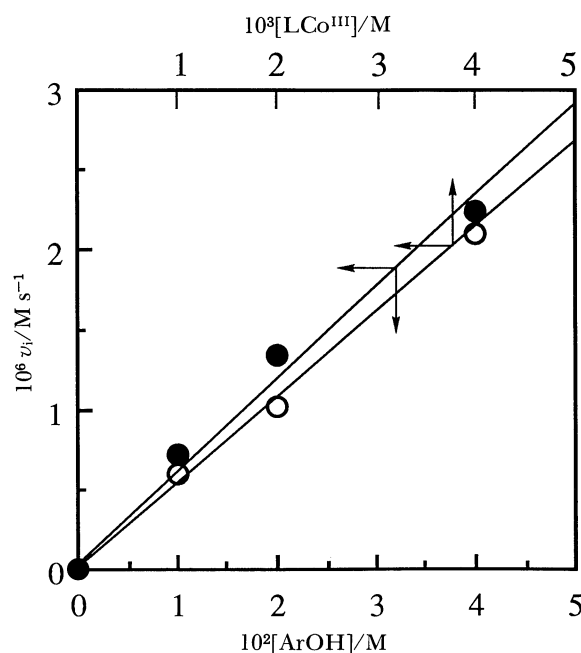


Fig. 9. Plots of initial rates (v_i) vs. initial concentrations of $[\text{Co}(\text{tip}(\text{b}))]^{2+}$ and 2,4-di-*t*-butylphenol (ArOH) concentrations with constant concentrations of the phenol (2.0×10^{-2} M) and $[\text{Co}(\text{tip}(\text{b}))]^{2+}$ (2.0×10^{-3} M) in Me₂CO under oxygen.

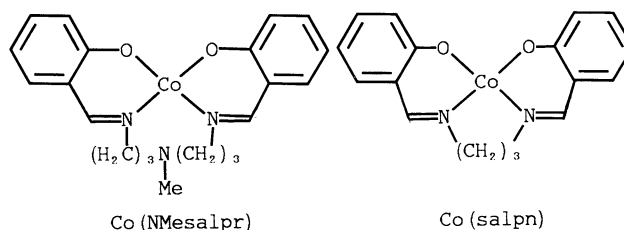
cobalt had completely disappeared early in the course of the reaction. It is evident that the present reaction does not involve hydrogen atom abstraction by the superoxide as rate-determining. Meanwhile, as Fig. 9 shows, the initial rates, which were calculated from a slope at time zero in an absorbance-time profile, were proportional to the added catalyst and phenol concentrations and dependent on the exerted oxygen pressure over the solution. Because of the complexity of the present system, no quantitative description of the concentration-dependency of the rate is attempted. In order to explain these results only qualitatively, therefore, we presents two assumptions that (1) the decomposition of III to *o*-BQ is virtually rate-determining and (2) the hydroxocobalt complex (LCoOH⁻) plays an important role as a limiting intermediate species in a catalytic cycle (Eqs. 4, 5, 6, and 7); the aforementioned finding that the amount of produced *o*-BQ increased linearly with reaction time evidences that the steady state is reached and thus the steady-state concentrations of the hydroxo complex and III must be kept constant during the course of the reaction. Since catalytic levels of III as well as the hydroxo complex or its precursor would rise with the increasing concentrations of the phenol, metal catalyst, and dissolved oxygen, the overall rate would increase accordingly, as was observed.

Meanwhile, product analysis for the catalytic oxygenation of 2,6-di-*t*-butylphenol,²⁸⁾ yielding 2,6-di-*t*-butyl-*p*-benzoquinone (*p*-BQ) and a diphenquinone

Table 4. Oxygenation of 2,6-Di-*t*-butylphenol ($\pm 2\%$ error in yield)^{a)}

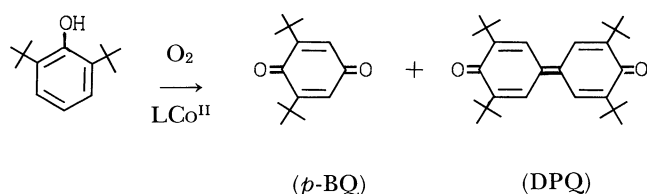
Catalyst	Solvent	Reaction time/h	Conversion/% ($\pm 3\%$)	<i>p</i> -BQ/DPQ
[Co(tip(b))] ²⁺	MeNO ₂	24	70	94/6
	Me ₂ C=O	24	67	96/4
	MeCN	24	51	93/7
	MeOH	24	49	86/14
	CH ₂ Cl ₂	24	10	78/22
	CHCl ₃	24	6	61/39
[Co(tip(d))] ²⁺	MeCN	24	12	86/14
[Co ₂ (tip(b)) ₂ (O ₂)] ⁴⁺	MeCN	24	21	81/19
Co(NMesalpr)	MeCN	1	100	100/0 ⁽³²⁾
	Toluene	6	100	100/0 ⁽³²⁾
Co(salpn)	CHCl ₃ -py	24	40	80/20 ⁽³²⁾

a) Conditions: substrate 0.5 mmol; catalyst 0.05 mmol in 25 ml solvent under an oxygen atmosphere at room temperature. NMesalpr: *N,N'*-disalicylidene-4-methyl-4-azaheptane-1,7-diamine; Salpn: *N,N'*-disalicylidene-1,3-propanediamine.



(DPQ),²⁹⁾ is somewhat instructive to implicate the reaction mechanism. The results obtained in this work are compared with reported literature data, which are also included in Table 4. Complete interpretation for these results is still rather difficult owing to a lack of available data. However, the mechanism analogous to that for 2,4-di-*t*-butylphenol seems most plausible; the reaction proceeds either via a radical pathway including a phenoxyl radical or via an ionic pathway involving the phenolato LCo^{III} complex.³⁰⁾ Several points about Table 4 are noteworthy; as with the case of 2,4-di-*t*-butylphenol, generally, use of polar solvents such as nitromethane and acetonitrile gave rise to better total yields and

cally binds Co²⁺ ion at a 1:1 ratio to form [Co(tip)]²⁺, which then immediately takes up molecular oxygen to form the cobalt-dioxygen complex entirely stable in the solid state and enough stable below -30°C in solution. As is visualized by the CPK space filling molecular model, [Co(tip)]²⁺ adopts a loose square-pyramidal geometry; ineffective interaction between the four equivalent imidazolyl nitrogen lone-pairs and the central metal cation causes elongation of the Co-N(py) bond to reduce the fifth coordination of the pyridyl nitrogen to the metal ion, which coordination appears to be a necessary prerequisite of oxygen fixation. In accord with this inference, the catalytic behavior of [Co(tip)]²⁺ differs greatly from those of tetra-coordinated Co(salen) in non-coordinating solvents and penta-coordinate Co(salpr), which selectively afford biphenyl-2,2'-diol and the *o*-quinone, respectively (Table 3). Thus, the catalytic behavior of [Co(tip)]²⁺ becomes intermediate between them. The present cobalt oxygen complex is unique in structure among oxygen complexes because it possesses four equal imidazolyl groups as peripheral ligands. However, it should be born in mind that our structural assignment is based on an only limited data. The O-O stretching frequencies of cobalt oxygen adduct has been the focus of recent studies since it is a measure of electron donating ability of the chelate. Therefore, resonance Raman or IR studies are under investigation for a detailed characterization of the Co-O and O-O bonding. The results will be published in the near future.



preferred formation of *p*-BQ over DPQ, since polar solvents would enhance the production of the metal-complexed phenolate [II₁] and hence would increase the contribution of the ionic process. Replacement of the alkyl group in the imidazolyl ligand with an electron-withdrawing methoxymethyl group diminishes the reducing ability of the central Co^{II} toward a phenoxyl radical, resulting in a higher yield of DPQ vs. *p*-BQ.³¹⁾

In conclusion, the pyridyl ligand symmetrically substituted with four imidazolyl groups stoichiometri-

References

- 1) T. Tumaki, *Bull. Chem. Soc. Jpn.*, **13**, 252 (1938).
- 2) L. Vaska, *Science*, **140**, 809 (1963); L. H. Vogt, H. M. Faigenbaum, and S. E. Wiberley, *Chem. Rev.*, **63**, 269 (1963); M. M. Taqui Khan and A. E. Martell, "Homogeneous Catalysis by Metal Complexes," Academic Press, New York (1974); E. C. Niederhoffer, J. H. Timmons, and A. E. Martell, *Chem. Rev.*, **84**, 137 (1984).
- 3) A. B. P. Lever and H. B. Gray, *Acc. Chem. Res.*, **11**, 348 (1978).
- 4) F. Basolo, B. M. Hoffman, and J. A. Ibers, *Acc. Chem. Res.*, **8**, 384 (1975); D. A. Summerville and F. Basolo, *Chem. Rev.*, **79**, 139 (1979); R. S. Drago, J. Gaul, A. Zombeck, and D. K. Straub, *J. Am. Chem. Soc.*, **102**, 1033 (1980); M. Suzuki, H. Kinatomi, and I. Murase, *Bull. Chem. Soc. Jpn.*, **57**, 36 (1984); A. E. Martell and R. J. Motekaitis, *J. Am. Chem. Soc.*, **110**, 8059 (1988).
- 5) M. Calligaris, G. Nardin, L. Randaccio, and A. Ripamonti, *J. Chem. Soc. A*, **1970**, 1069.
- 6) C. Floriani and F. Calderazzo, *J. Chem. Soc. A*, **1969**, 946.
- 7) A. L. Crumbliss and F. Basolo, *J. Am. Chem. Soc.*, **92**, 55 (1970); G. A. Rodley and W. T. Robinson, *Nature (London)*, **235**, 438 (1972).
- 8) J. H. Wang, *J. Am. Chem. Soc.*, **80**, 3168 (1958); J. P. Collman, R. R. Gagne, C. A. Reed, T. R. Halbert, G. Lang, and W. T. Robinson, *J. Am. Chem. Soc.*, **97**, 1427 (1975).
- 9) R. A. Sheldon and J. K. Kochi, "Metal-Catalyzed Oxidations of Organic Compounds," Academic Press, New York (1981), Chap. 4; W. K. Seok and T. J. Meyer, *J. Am. Chem. Soc.*, **110**, 7358 (1988).
- 10) M. J. Barnes, R. S. Drago, and K. J. Balkus, Jr., *J. Am. Chem. Soc.*, **110**, 6780 (1988). R. J. Motekaitis and A. E. Martell, *ibid.*, **110**, 7715 (1988).
- 11) S. Takano, Y. Yano, and W. Tagaki, *Chem. Lett.*, **1981**, 1177.
- 12) Y. Sasagawa, "Wargburg's Manometric Method," Jikken Kagaku Koza, Maruzen, Tokyo (1958), Vol. 24, p. 86.
- 13) K. Ley and E. Müller, *Chem. Ber.*, **89**, 1402 (1956).
- 14) E. Müller and K. Ley, *Chem. Ber.*, **88**, 601 (1955).
- 15) M. S. Kharasch and B. S. Joshi, *J. Org. Chem.*, **22**, 1439 (1957).
- 16) M. J. Carter, D. P. Rillema, and F. Basolo, *J. Am. Chem. Soc.*, **96**, 392 (1974).
- 17) G. Tautzher, G. Amiconi, E. Antonini, M. Brunori, G. Antonini, and G. Costa, *Nature (London)*, **241**, 222 (1973).
- 18) J. C. Stevens and D. H. Busch, *J. Am. Chem. Soc.*, **102**, 3285 (1980).
- 19) A. E. Martell, *Acc. Chem. Rec.*, **15**, 155 (1982).
- 20) M. S. Calvin, R. H. Bailes, and W. K. Wilmarth, *J. Am. Chem. Soc.*, **68**, 2254 (1946).
- 21) B. M. Hoffman, D. L. Diemente, and F. Basolo, *J. Am. Chem. Soc.*, **92**, 61 (1970).
- 22) G. McLendon, S. R. Pickens, and A. E. Martell, *Inorg. Chem.*, **16**, 1551 (1977).
- 23) A. Nishinaga and H. Tomita, *J. Mol. Catal.*, **7**, 179 (1970).
- 24) A. Nishinaga, H. Tomita, K. Nishizawa, and T. Matsuura, *J. Chem. Soc., Dalton Trans.*, **1981**, 1506.
- 25) R. R. Grinstead, *Biochemistry*, **3**, 1308 (1964); C. R. H. I. de Jonge, "Organic Syntheses by Oxidation with Metal Compounds," ed by W. J. Mills and C. R. H. I. de Jonge, Plenum Press, New York (1986), p. 473.
- 26) A. Nishinaga, H. Iwasaki, T. Kondo, and T. Matsuura, *Chem. Lett.*, **1985**, 5; A. Nishinaga, H. Tomita, and T. Matsuura, *ibid.*, **1979**, 2893.
- 27) D. D. Cox and L. Que, Jr., *J. Am. Chem. Soc.*, **110**, 8085 (1988).
- 28) V. Kothari and J. J. Tazuma, *J. Catal.*, **41**, 180 (1976); H. M. van Dort and H. J. Geursen, *Recl. Trav. Chim. Pay-Bas*, **86**, 520 (1967).
- 29) L. H. Vogt, J. G. Wirth, and H. L. Finkbeiner, *J. Org. Chem.*, **34**, 273 (1969); A. S. Hay, *ibid.*, **34**, 1160 (1969).
- 30) D. L. Tomaja, L. H. Vogt, and J. G. Wirth, *J. Org. Chem.*, **35**, 2029 (1970); A. Nishinaga, H. Tomita, K. Nishizawa, and T. Matsuura, *J. Chem. Soc., Dalton Trans.*, **1981**, 1504.
- 31) D. L. Tomaja, H. L. Vogt, and J. G. Wirth, *J. Org. Chem.*, **35**, 2029 (1970).
- 32) M. Frostin-Rio, D. Pujol, C. Bied-Charreton, M. Perrée-Fauvet, and A. Gaudemer, *J. Chem. Soc., Perkin Trans. 1*, **1984**, 1971.